Glass-formation and hardness of Cu-Y alloys

Journal of Alloys and Compounds 483 (2009) 50–53
doi:10.1016/j.jallcom.2008.07.148

Glass-formation and hardness of Cu–Y alloys

Marta Satta, Paola Rizzi, Marcello Baricco
Journal of Alloys and Compounds 483 (2009) 50–53
doi:10.1016/j.jallcom.2008.07.148

Abstract
Metallic glasses exhibit particularly attractive mechanical properties, like high stresses to fracture and large elastic strain (up to 2%), but they show generally low plasticity. Aim of this work is to investigate the glass forming range in the Cu–Y system, in order to form the ductile CuY phase (CsCl structure) upon crystallization. Cu58Y42, Cu50Y50 and Cu33Y67 alloys have been prepared by rapid solidification and copper mould casting, obtaining ribbons and cylindrical shaped ingots, with diameter of 2mm. Fully amorphous, partially amorphous and fully crystalline samples have been obtained for different compositions and quenching conditions. In some cases, the X-ray diffraction results, analysed using the Rietveld method, showed CuY nanocrystals embedded in an amorphous matrix. The microstructure was studied by transmission electron microscopy (TEM) and the presence of nanocrystals of the ductile phase CuY has been confirmed. Microhardness results showed a softening of the amorphous phase due to the presence of CuY nanocrystals and a hardening due to the Cu2Y phase.

1. Introduction

Many intermetallic compounds (e.g. NiAl, Ni3Al, FeAl) have low density, good oxidation resistance and high strength and stiffness at elevated temperature. This combination of properties makes them potentially useful for engineering applications. However, applications of polycrystalline intermetallics are severely limited by their poor ductility and low fracture toughness at ambient temperature [1]. High ductility was recently discovered in polycrystalline B2 (CsCl type structure) intermetallic compounds with the RM composition (where R is Y or a rare-earth element andMis a transition metal) [2]. Nearly all of the RM compounds are line compounds with exact 1:1 stoichiometry. Over 120 of such alloys exist and most of them exhibit good ductility. The most ductile composition reported, YAg, shows >20% elongation for polycrystalline specimen tested under tension at ambient temperature in room air of normal humidity [3]. The YCu and DyCu intermetallics are almost as ductile as YAg, with reported tensile elongation of 11% and 16%, respectively [4]. The glass forming ability in the Cu–Y system has been investigated and some amorphous alloys have been prepared by the melt spinning technique [5]. The microstructure of rapidly solidified Cu–Y alloys has been investigated by TEM [6]. Melt-spun Cu87Y13 alloy showeda veryfineeutectic of f.c.c. copper and hexagonalCu5Y, plus isolated areas of a new metastable orthorhombic phase, Cu9Y. Melt-spun Cu49Y51 alloy contained an amorphous matrix with precipitates of the equilibrium orthorhombic Cu2Y phase. Considering far from eutectic compositions, glass formation was obtained in the melt-spun Cu75Y25 alloy, but the melt-spun Cu58Y42 showed an ultrafine Cu2Y single phase. While high glass formability has been reported for some compositions corresponding to

intermetalliccompounds in the Cu–Ti and Cu–Zr system[7–9], it appears quite difficult to form a glass in the Cu–Y system [6]. Aim of this work is to investigate the glass formation in the Cu–Y system, in order to obtain the CuY phase (CsCl structure) upon crystallization. In fact, nanocrystals of the ductile phase embedded in an amorphous matrixmay enhance the plastic deformation of the glass [10].Nanosized precipitates are able to hinder the shear bands propagation and a stronger increase of plasticity is expected if the precipitates are constituted of an intrinsic ductile phase.

2. Experimental

Master alloys, corresponding to two eutectic compositions (Cu58Y42 and Cu33Y67) and a line compound Cu50Y50,were prepared from high purity Cu (99.99%) and Y (99.99%) by arc-melting under Ar atmosphere. Ribbonswere prepared by melt spinning, re-melting master alloys in a quartz crucible and ejecting the melt on a Cu-wheel rotating with a surface velocity of 35 (spin1) and 50 (spin2) m/s. Ingots cylinder (bulk)were also produced by casting the liquid alloy into a cylinder shaped (2mm diameter) copper mold. The samples were analysed by X-ray diffraction with Cu K_ radiation, using a standard Bragg–Brentano diffractometer. Experimental data have been analysed by the Rietveld method, using MAUD software [11], obtaining structural and microstructural parameters. Transmission electron microscopy (TEM) investigation was performed on a JEOL 2010 microscope operating at 200 kV. The samples were prepared using ion milling (4 kV, 1 A). Differential scanning calorimetry (DSC), under flowing argon and with a heating rate of 20 K/min, was used to characterize the crystallization process. The Vickers microhardness (Hv)was determined for ribbons and bulk samples by using 50 gf load and 100 gf load, respectively. Before testing, the samples surfaces were grinded with very fine grade papers in order to obtain flat surfaces.

3. Results and discussion

Cu58Y42, Cu33Y67 and Cu50Y50 samples have been studied by XRD and results are reported in Figs. 1 and 2, concerning ribbons and bulk samples, respectively. A careful Rietveld analysis of diffraction patterns allowed the determination of lattice constants, the volume fraction of phases and the coherent domain scattering (C.D.S.). For partially amorphous samples, the amorphous contribution has been treated as a background function (Gaussian peaks) and so the volume fraction of the phases have not been calculated. All the results are reported in Table 1. The pattern of spin1-Cu58Y42 (Fig. 1, curve I) shows the presence of a mixture formed by the CuY and the Cu2Y phases. The pattern related to spin2-Cu58Y42, obtained with a higher quenching rate, (Fig. 1, curve II), shows an amorphous halo, together with the presence of diffraction peaks due to the CuY phase. Concerning the composition of Cu33Y67, the XRD patterns of ribbons (Fig. 1, curves III and IV) show that with a low wheel velocity (spin1-Cu33Y67, curve III) it was possible to obtain an amorphous halo with the presence of the Y phase, with a preferred orientation along [0 0 1] direction. At higher wheel velocity (spin2-Cu33Y67) halos due to an amorphous phase can be observed in the pattern (Fig. 1, curve IV), even if weak peaks of unknown phases can be barely evidenced. It was not possible to obtain an amorphous phase for the Cu50Y50 composition, even with the highest wheel velocity. In fact spin2-Cu50Y50 (curve V) shows only the presence of the CuY phase. Fig. 2 shows that, for all compositions, it was not possible to obtain bulk amorphous samples. The pattern of bulk-Cu58Y42 is reported in curve I and the peaks are assigned to amixture formed by CuY and Cu2Y phases. For bulk-Cu33Y67 (curve II), the mixture is formed by CuY and Y phases. Only the peaks corresponding to the CuY phase (curve III) were observed for bulk-Cu50Y50. For the investigatedribbons, the lattice parameters remains similar to those of themaster alloys (not reportedinTable 1), suggesting that there were not an enhancement of

dissolution of elements in the intermetallics compounds due to rapid solidification. The values of C.D.S. decrease from bulk to ribbons, because of the effect of the cooling rate. Only for Cu50Y50 a higher C.D.S. was observed for ribbon with respect to the bulk sample, likely because of the high growth rate of the compound in undercooling conditions. As it was expected, for all samples the volume fraction of the phases is close to the percentage of the equilibrium phases. The microstructure of spin2-Cu58Y42 is shown in Fig. 3a, where a TEM bright-field image is reported. The presence of spherical shaped nanosize crystals, with dimension up to 20 nm, of the CuY phase (identified in the SAD),embedded in an amorphous matrix, is observed. InFig. 3b the microstructure of spin1-Cu58Y42 is reported, in which coarser crystals of eutectic CuY and Cu2Y phases (identified in the SAD) are embedded in an amorphous matrix. The average size of the eutectic nodules is in the range from 10 to 50 nm. This result is comparable with that obtained with the Rietveld analysis (Table 1), where the value of the coherent domain scattering of the CuY phase is 31 nm, while for the Cu2Y phase is 18 nm. The crystallization process of the amorphous phases was analyzed by DSC and the corresponding thermograms of as-quenched ribbons are reported in Fig. 4. Spin1-Cu58Y42 (curve a) shows a large exothermic peak with Tx = 527K and $\_Hx$ = 3.1 kJ/mol, confirming the presence of an amorphous fraction in the sample. Spin2-Cu58Y42 (curve b) exhibits a main exothermic peak, starting at about 505K with $\_Hx$ = 3.3 kJ/mol. For a better understanding of the crystallization process, spin2-Cu58Y42 was annealed up to 500 and 575K and the corresponding XRD patterns are reported in Fig. 5 curves I and II, respectively. From the XRD pattern obtained after annealing up to 500K, CuY crystals with C.D.S of 27nm were observed, comparable to the C.D.S. of the quenched-in crystals, together with Cu2Y nanocrystals (C.D.S. = 6 nm) nucleated from the amorphous phase. After annealing at 575K (end of the crystallization peak) the crystals reach C.D.S. values of 13nm (Cu2Y) and 34nm (CuY), respectively, because of the growth process. The DSC thermogramobtained for spin1-Cu33Y67 (Fig. 4, curve c) shows a single exothermic peak starting at 510K, with an enthalpy of crystallization ($\_Hx$) of 4.2 kJ/mol. Similarly, the DSC trace for spin2-Cu33Y67 (Fig. 4, curve d) consists of a main crystallization peak starting around 520K with a $\_Hx$ = 4.6 kJ/mol, and few exothermic peaks in the temperature range 580–680 K, in good agreement with the results ($\_Hx$ = 4.4 kJ/mol) reported in Ref. [5]. The results for spin1 and spin2-Cu33Y67 are very similar, because the fraction of the crystalline phase is very low. The Vickers microhardness test has been used to estimate the mechanical properties and the results are reported in Table 1. The Hv values for spin1-Cu33Y67 and spin2-Cu50Y50 are not reported because the ribbonswere too thin and tight that itwas not possible to perform the hardness test. Spin1-Cu58Y42 is constituted by an amorphous phase with nanocrystals of CuY and Cu2Y phase, which lead to a hardness value of 4.11 GPa. The C.D.S. values of CuY and Cu2Y phases in bulk- Cu58Y42 are higher than in spin1-Cu58Y42, so that the hardness value becomes lower (3.04GPa). In addition, in the bulk sample there is not the contribution to the hardness due to the amorphous phase. Spin2-Cu58Y42 as-quenched sample shows a lower Hv value (2.08 GPa), because of the absence of the Cu2Y phase. The Hv value increases in the annealed samples up to 2.55 GPa (500K) and 2.91GPa (575 K) because of the increasing fraction of the Cu2Y phase. Therefore, nanocrystals of the Cu2Y phase leads to hardening in the material, while lower hardness values are observed when the samples contains only the amorphous and the CuY phases. Spin2-Cu33Y67 shows a higher hardness value (2.69 GPa) with respect to the bulk-Cu33Y67 (2.37GPa), as expected for an amorphous sample with respect to the corresponding crystalline counterparts (CuY and Y). From the microhardness value obtained for bulk-Cu50Y50 (3.04GPa) and using the Tabor relationship (_f = 1/3 Hv) [12], a fracture yield of about 1000MPamay be envisaged. This value is much higher with respect to that obtained from tensile test in polycrystalline material (200MPa) [4]. This discrepancy might be attributed to the presence of

microcracks in the polycrystalline sample, which leads to a low apparent strength [4]. In addition, the occurrence of a small C.D.S. in the bulk-Cu50Y50 sample (40 nm) might contribute to an increase in the hardness.

4. Conclusions

CuxY1−x alloys (x = 33, 50 and 58) have been prepared by melt spinning and copper mould casting, obtaining ribbons and bulk samples. Crystallization of amorphous phases has been followed by DSC. Hardness test has been usedfor estimatingmechanical properties. Using a Rietveld refinement of XRD patterns, C.D.S. valueswere estimated and their influence on hardness was described. Only for melt-spun Cu33Y67 a fully amorphous phase has been produced. For Cu58Y42 and Cu50Y50, partially amorphous and fully crystalline ribbons have been obtained, respectively. Equilibrium phases were obtained in bulk samples. CuY phase embedded in an amorphous matrix leads to a low value of hardness, suggesting a possible increase in the plasticity of the glassy phase. On the contrary, the presence of the Cu2Y phase leads always to a hardening of thematerials. The presence of coarsegrained crystals decreases the hardness values.

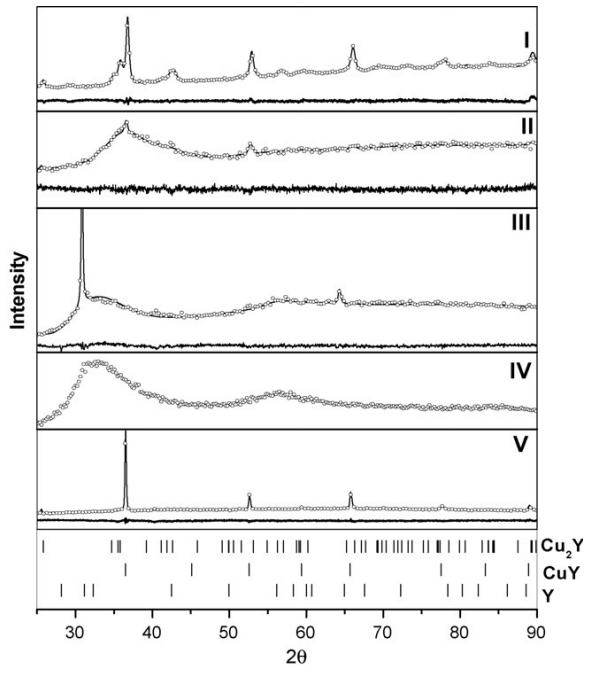

Fig. 1. X-ray diffraction of as-quenched ribbons for spin1-Cu58Y42 (curve I), spin2-Cu58Y42 (curve II), spin1-Cu33Y67 (curve III), spin2-Cu33Y67 (curve IV) and spin2-Cu50Y50 (curve V). Selected points (circles) and calculated pattern (continuous line) are reported. When available, the difference between experimental data and the pattern calculated from the Rietveld analysis is reported.

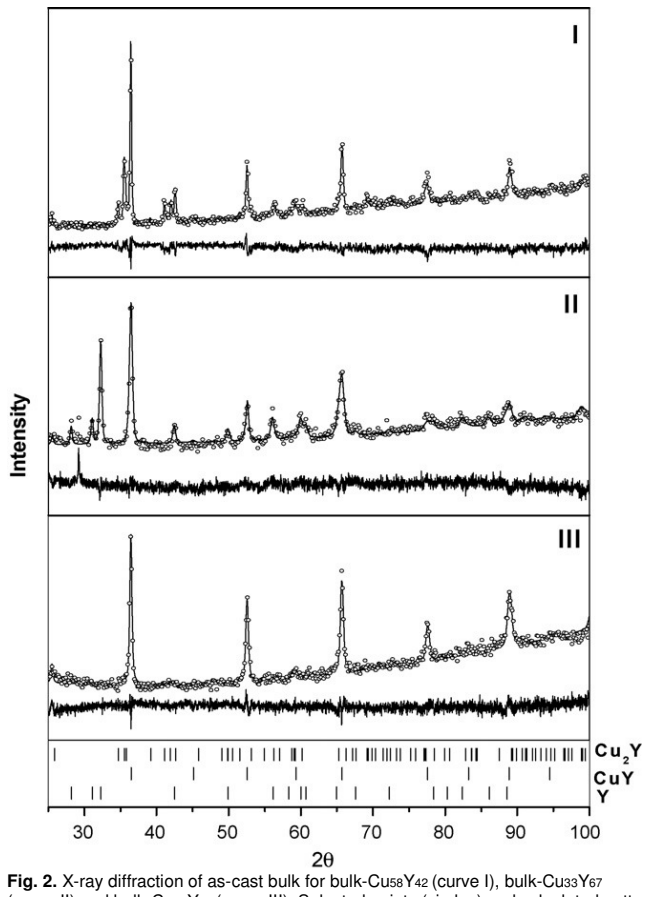

Fig. 2. X-ray diffraction of as-cast bulk for bulk-$Cu_{58}Y_{42}$ (curve I), bulk-$Cu_{33}Y_{67}$ (curve II) and bulk-$Cu_{50}Y_{50}$ (curve III). Selected points (circles) and calculated pattern (continuous line) are reported. The difference between experimental data and the pattern calculated from the Rietveld analysis is reported.

Table 1
Results of Rietveld analysis of XRD patterns: *a*, *b* and *c* are lattice constants; C.D.S. is the size of the coherent domain scattering; % is the phase fraction. Hv is the hardness
obtained from Vickers indentation measurements.

	CuY			Cu_2Y			Y			Hv (GPa)
	a (Å)	C.D.S. (nm)	%	*a* (Å)	*b* (Å)	*c* (Å)	C.D.S. (nm)	%	*a* (Å)	*c* (Å)	C.D.S. (nm)	%	
Spin-$Cu_{58}Y_{42}$	1	3.4702	31	54	4.2861	6.8867	7.3078	18	46	4.11	?0.18		
Spin-$Cu_{58}Y_{42}$	2	3.4549	28	–	2.08	?0.15							
Spin-$Cu_{33}Y_{67}$	1	3.6227	5.7887	45	–	–							
Spin-$Cu_{33}Y_{67}$	2	2.69	?0.17										
Spin-$Cu_{50}Y_{50}$	2	3.4772	106	100	–								
Bulk-$Cu_{58}Y_{42}$		3.4771	54	52	4.2922	6.8925	7.3093	84	48	3.04	?0.06		
Bulk-$Cu_{33}Y_{67}$		3.4756	37	66	3.6563	5.7561	40	34	2.37	?0.08			
Bulk-$Cu_{50}Y_{50}$		3.4778	40	100	2.13	?0.21							
Spin2-$Cu_{58}Y_{42}$													
500K		3.4699	27	–	4.2792	6.9253	7.3221	6	–	2.55	?0.22		
575K		3.4718	34	–	4.2753	6.8941	7.3295	13	–	2.91	?1.11		

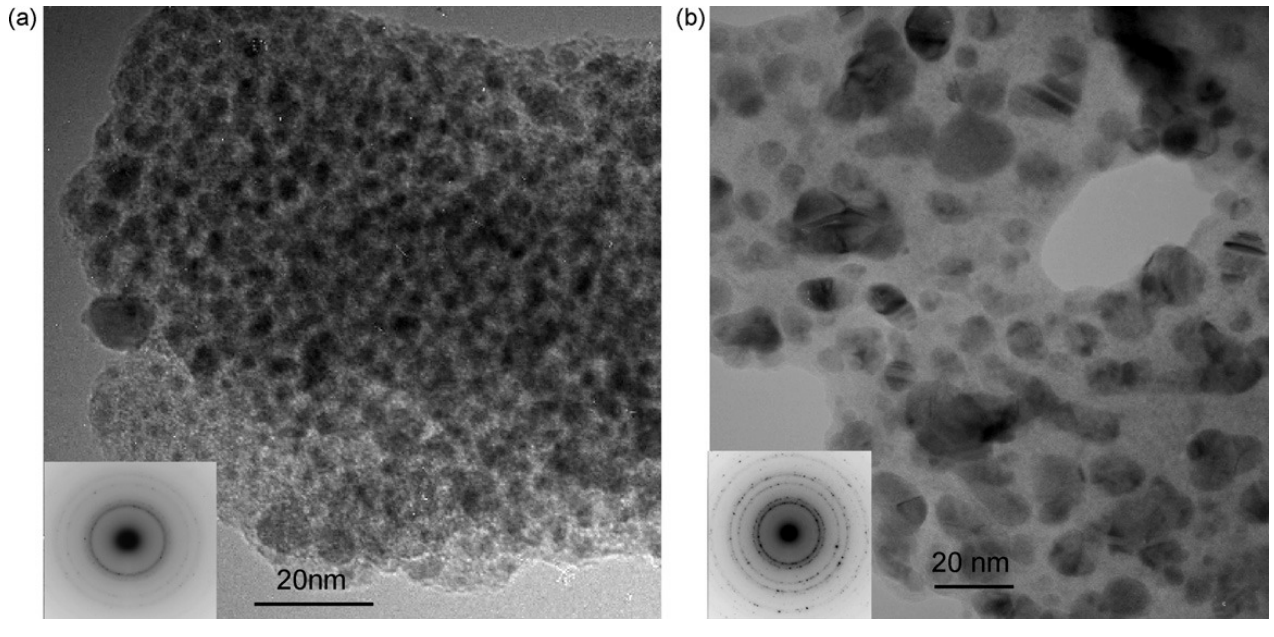

Fig. 3. TEM picture of (a) spin2-$Cu_{58}Y_{42}$ and (b) spin1-$Cu_{58}Y_{42}$

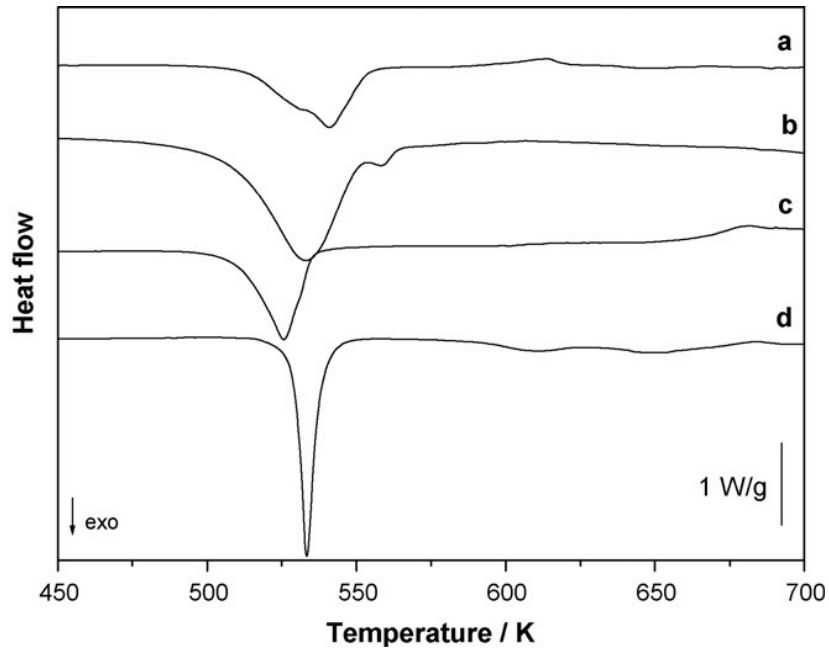

Fig. 4. DSC curves, obtained with an heating rate of 20 K/min, for as-quenched ribbons: (a) spin1-$Cu_{58}Y_{42}$, (b) spin2-$Cu_{58}Y42$, (c) spin1-$Cu_{33}Y_{67}$ and (d) spin2-$Cu_{33}Y_{67}$.

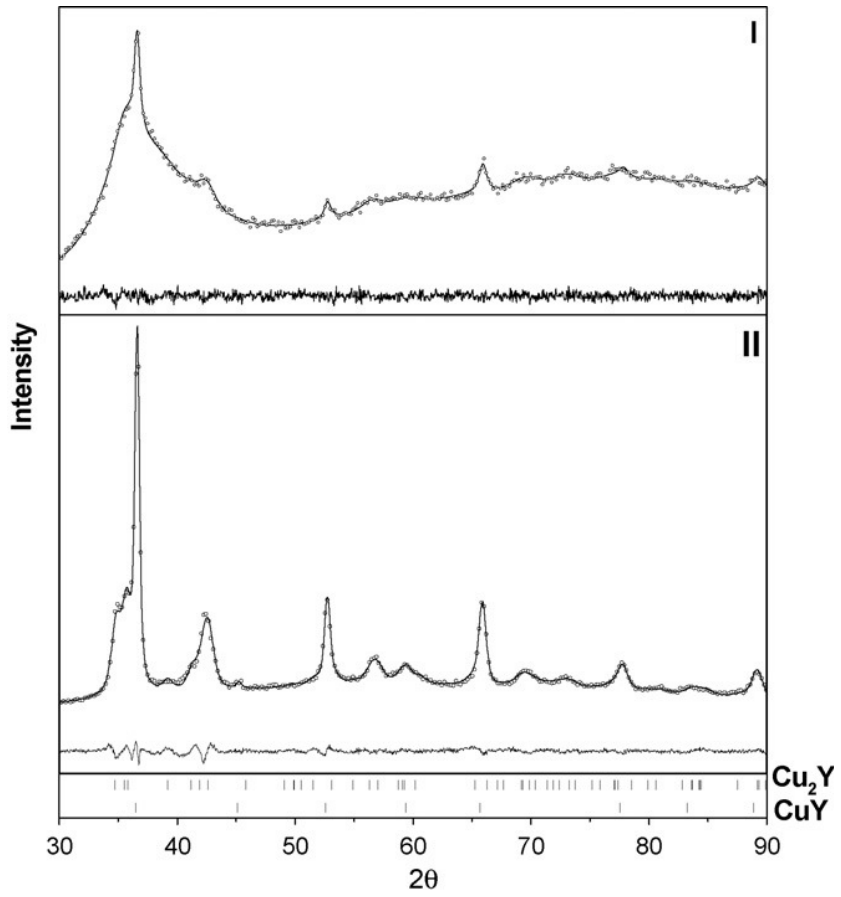

Fig. 5. X-ray diffraction patterns of spin2-$Cu_{58}Y_{42}$ annealed up to 500K (curve I) and up to 575K (curve II). Selected points (circles) and calculated pattern (continuous line) are reported. The difference between experimental data and the pattern calculated from the Rietveld analysis is reported.

Acknowledgements

The authors acknowledge financial support from Regione Piemonte (Progetto D23 and Progetto NANOMAT-Docup 2000–2006, Linea 2.4a), MIUR (Progetto COFIN/MIUR 2005- 097983 002) and European Community (Project MCRTN-CT-2003- 504692).

References

[1] A.M. Russell, Adv. Eng. Mater. 5 (2003) 629.

[2] K.A. Gschneidner, A.M. Russell, A.O. Pecharsky, J.R. Morris, Z. Zhang, T.A. Lograsso, D. Hsu, C.C.H. Lo, Y. Ye, A. Slager, D. Kesse, Nat. Mater. 2 (2003) 587.

[3] A.M. Russell, Z. Zhang, T.A. Lograsso, C.C.H. Lo, A.O. Pecharsky, J.R. Morris, Acta Mater. 52 (2004) 4033.

[4] Z. Zhang, A.M. Russell, S.B. Biner, K.A. Gschneidner, C.C.H. Lo, Intermetallics 13 (2005) 559.

[5] K. Jansson, M. Nygren, J. Less Common Met. 128 (1987) 319–329.

[6] X. Zhang, A. Atrens, J. Mater. Sci. 28 (1993) 6809.

[7] J. Reeve, G.P. Gregan, H.A. Davies, in: S. Steeb, H. Warlimont (Eds.), Rapidly QuenchedMetals V, Proceedings of the 5th International Conference on Rapidly Quenched Metals (RQ5), Elsevier, Amsterdam, 1985, p. 203.

[8] E. Kneller, Y. Khan, U. Gorres, Z. Metallkde 77 (1986) 152.

[9] R.C. Budhani, T.C. Goel, K.L. Chopra, in: T. Masumoto, K. Suzuki (Eds.), Rapidly Quenched Metals IV, Proceedings of the 4th International Conference on Rapidly Quenched Metals (RQ4), Japan Institute of Metals, 1982, p. 615.
[10] W.L. Johnson, MRS Bull. 24 (10) (1999) 42.
[11] MAUD is a Rietveld software developed by L. Lutterotti, University of Trento, Italy (www.ing.unitn.it/□luttero/maud).
[12] G.E. Dieter, Mechanical Metallurgy, 3rd ed., McGraw-Hill Book Company, London, UK, 1988, p. 330.